doi: 10.15407/ujpe61.08.0681

I.O. ANISIMOV, M.A. SHCHERBININ

Taras Shevchenko National University of Kyiv,
Faculty of Radiophysics, Electronics, and Computer Systems
(4G, Academician Glushkov Ave., Kyiv 03022, Ukraine)

DYNAMICS OF SHORT ELECTRON BUNCHES AND WAKEFIELDS EXCITED BY THEM IN PLASMA WITH AND WITHOUT A LONGITUDINAL MAGNETIC FIELD

PACS 52.35.Fp, 52.40.Mj, 52.65.Rr

Using the computer simulation, the influence of a longitudinal magnetic field on the wakefield excitation in plasma by an initially cylindrical electron bunch with the length equal to the wake wavelength and the inverse influence of excited fields on the bunch dynamics have been considered. It is shown that the magnetic field can suppress the radial defocusing of the bunch and increase the length of the region, in which the wake waves are excited, as well as the amplitude of those waves.

K e y w o r d s: plasma, electron bunch, longitudinal magnetic field, wakefield, radial defocusing of a bunch.

1. Introduction

The problem of wakefield excitation by electron bunches and the inverse influence of this field on the bunch dynamics is of interest, first of all, from the viewpoint of whether it is possible to create a compact electron accelerator based on wake waves. A capability of wakefield excitation in plasma (see, e.g., [1, 2]) and insulators (see, e.g., [3, 4]) is discussed in the literature. Electron and ion bunches, or the sequences of such bunches [5–10], as well as short ultra-powerful laser pulses [11], can be used as a tool for the wakefield excitation. A possibility of construction of wakefield accelerators was confirmed experimentally (see, e.g., [12]). In recent laser experiments [13], the scientists were enabled to obtain a beam with an energy of a few GeV. The simulation testifies that the electron bunches that arise under the action of a laser pulse [14] can also make a contribution to the formation of wakefields in such systems. The problem of wakefield excitation is also interesting owing to a possibility of inhomogeneous plasma diagnostics through the analysis of the transition radiation emitted by charged particles and bunches [15], as well as owing to their capability to focus electron bunches [16].

Among the problems that arise at the wakefield excitation by electron bunches, there is the radial defocusing of the latter under the action of the fields excited by themselves. This defocusing can be prevented, by imposing a longitudinal magnetic field on the system [17]. In this work, the dynamics of short (with the length equal to the wake wavelength), initially cylindrical electron bunches injected into a homogeneous plasma along the external uniform magnetic field is considered in detail. For comparison, a similar system, but without magnetic field, is also analyzed. The main aim of the work consisted in elucidating the mechanisms of bunch focusing-defocusing and the focusing action of the magnetic field.

The wakefields excited by an electron bunch in plasma were studied analytically and with the help of numerical simulations. The analytical calculation was carried out in the linear approximation. The in-

verse influence of the beam-excited wakefields on the beam motion was neglected. The numerical calculation was performed using the PIC method.

2. Analytical Calculation of Wakefield Excitation

Let a cylindrical bunch with the radius r_0, length L, and charge density n_{B0} move in a homogeneous warm plasma with the concentration n_0 and the temperature T at the velocity v_0 directed along the bunch axis:

$$n_B(\mathbf{r},t) = n_B(r,\xi) = \begin{cases} n_{B0},\ r \le r_0 \cap |\xi| \le L/2; \\ 0,\ r > r_0 \cup |\xi| > L/2, \end{cases} \quad \xi = z - v_0 t \tag{1}$$

(the axis z of the cylindrical coordinate system is directed along the bunch axis). The magnetic field is absent. Plasma ions are considered to be motionless, and the bunch shape to be fixed. The inverse influence of the wakefields excited by the bunch on the bunch itself is neglected.

The motion of plasma under the action of the bunch-generated electric field is described by a system of the motion and continuity equations and the Gauss theorem:

$$\begin{aligned} &mn\frac{d\mathbf{v}}{dt} = -en\mathbf{E} - \nabla p - mn\nu\mathbf{v}; \\ &\frac{\partial n}{\partial t} + \nabla(n\mathbf{v}) = 0; \\ &\nabla\mathbf{E} = -4\pi e(n_1 + n_B), \end{aligned} \tag{2}$$

where $p = nk_BT$ is the pressure of the electron gas, $n = n_0 + n_1(\mathbf{r},t)$ is the perturbed plasma density, $\mathbf{v}(\mathbf{r},t)$ is the plasma velocity, and ν is the frequency of electron collisions with heavy particles.

By linearizing system (2) in the case of the small magnitudes of n_1 and $\mathbf{v}$, it can be reduced to a wave equation in the form

$$v_{Te}^2\Delta n_1 - \frac{\partial^2 n_1}{\partial t^2} - \nu\frac{\partial n_1}{\partial t} - \omega_p^2 n_1 = \omega_p^2 n_B. \tag{3}$$

Making the automodel substitution (see Eq. (1)) in the wave equation (3) and taking the axial symmetry of the problem into account, we obtain

$$\frac{v_{Te}^2}{r}\frac{\partial}{\partial r}\left[r\frac{\partial n_1(r,\xi)}{\partial r}\right] + \left(v_{Te}^2 - v_0^2\right)\frac{\partial^2 n_1(r,\xi)}{\partial\xi^2} + \nu v_0\frac{\partial n_1(r,\xi)}{\partial\xi} - \omega_p^2 n_1(r,\xi) = \omega_p^2 n_B(r,\xi). \tag{4}$$

Let us seek the solution of Eq. (4) with the help of the Fourier transformation (with respect to ξ) and the Fourier–Bessel one (with respect to r). The spatial spectrum of the plasma density perturbation, which emerges owing to the excitation of wake waves, looks like

$$n_1\left(k_\perp, k_\parallel\right) = -n_{B0}\sin\frac{k_\parallel L}{2}\,J_1\left(k_\perp r_0\right)\left(\pi k_\parallel k_\perp\right)^{-1} \times \left[k_\perp^2 r_D^2 + k_\parallel^2 r_D^2\left(1-\beta^2\right) + 1 - ik_\parallel r_D\beta s\right]^{-1}. \tag{5}$$

Here, the wave numbers $k_\parallel$ and $k_\perp$ correspond to the relevant transformations with respect to ξ and r, respectively. We took into account that $r_D = v_{Te}/\omega_p$ and used the notations $\beta = v_0/v_{Te}$ and $s = \nu/\omega_p$. The $k_\parallel$-roots of the denominator in Eq. (5) are calculated by the formula

$$k_{\parallel 1,2} = \frac{-i\beta s \pm \sqrt{(\beta^2-1)(1+k_\perp^2 r_D^2) - \beta^2 s^2}}{2r_D(\beta^2-1)} = \pm k_\parallel' - ik_\parallel''. \tag{6}$$

There is no singularity at the point $k_\parallel = 0$. One can see that both poles are located in the lower half-plane of the complex plane $\{\mathrm{Re}\,k_\parallel, \mathrm{Im}\,k_\parallel\}$.

The inverse Fourier transformation of the spatial spectrum (5) with respect to $k_\parallel$ can be performed, by using the residual method according to the Jordan lemma,

$$\begin{aligned} n_1(k_\perp,\xi) = &-\frac{n_{B0}J_1(k_\perp r_0)\exp\left(k_\parallel''\xi\right)}{2\pi r_D^2(\beta^2-1)k_\perp k_\parallel' k'} \times \\ &\times\left(\theta\left(\frac{L}{2}-\xi\right)\exp\left(k''\frac{L}{2}\right)\cos\left[k_\parallel'\left(\xi-\frac{L}{2}\right)+\psi\right] - \right. \\ &\left. -\,\theta\left(\frac{L}{2}-\xi\right)\exp\left(-k''\frac{L}{2}\right)\cos\left[k_\parallel'\left(\xi+\frac{L}{2}\right)+\psi\right]\right), \\ k' = &\sqrt{\left(k_\parallel'\right)^2 + \left(k_\parallel''\right)^2}, \\ \psi = &\,\mathrm{arctg}\frac{k_\parallel''}{k'}, \end{aligned} \tag{7}$$

where $\theta(x)$ is the Heaviside function. One can see that the wakefield is absent in front of the bunch ($\xi > L/2$) and vanishes at $\xi \to -\infty$, i.e. behind the bunch, because of collisions.

Ultimately, the distribution $n_1(r,\xi)$ can be obtained in the coordinate system moving with the

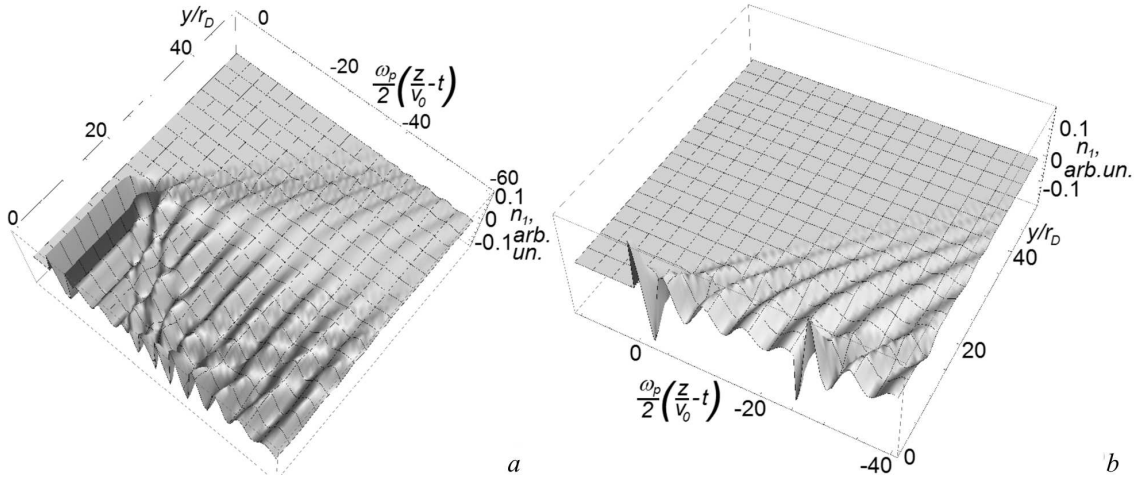

Fig. 1. Perturbation of the background plasma density by a cylindrical bunch at $B = 0$: (a) $r_0/r_D = 20$ and $L/r_D = 6$, (b) $r_0/r_D = 2$ and $L/r_D = 25$. Calculations were carried out in the linear approximation in the coordinate system moving with the bunch

bunch, by applying the inverse Fourier–Bessel transformation to Eq. (7):

$$n_1(r,\xi) = \int_0^\infty n_1(k_\perp,\xi) J_0(k_\perp r)\, k_\perp dk_\perp. \tag{8}$$

Integral (8) was calculated numerically. The corresponding results obtained for the characteristic values of model parameters are shown in Fig. 1.

In the cold plasma model, the wake waves can be excited only in the plasma region, where the charged bunch has passed [18]. Taking the nonzero plasma temperature into account results in that the boundary of this region, in accordance with the Huygens–Fresnel principle, becomes a source of secondary waves. Those waves propagate both toward the nonperturbed plasma and into the region, where the bunch is moving, and affect, in particular, the field near the axis of the examined system (Fig. 1, a). In addition, for thin (on the scale of Debye radius r_D) bunches, the variation of the wakefield at the axis can be induced by the radiation damping owing to the emission of Langmuir waves (Fig. 1, b). For wide bunches, the wake field is mainly concentrated in the region, through which the electron bunch passes, even in a warm plasma (Fig. 1, a).

3. Model Parameters

As was already mentioned, the analytical calculation presented above does not make allowance for the inverse influence of the wakefields excited by the bunch on the bunch itself. This influence can be taken into account with the help of a computer-assisted simulation within the PIC method. We use the electromagnetic relativistic code described in [19]. The simulated cylindrical volume had a length of 1.5 m and a radius of 0.2 m. The background plasma was characterized by a density of 5×10^8 cm^{-1} (the Langmuir frequency $\omega_p = 12.5 \times 10^8$ s^{-1}), the temperatures of electrons and ions were equal to 2 eV (the electron Debye radius $r_D = 5$ mm) and 0.2 eV, respectively. The longitudinal magnetic field was equal to zero or $B = 1$ mT, which corresponded to the electron cyclotron frequency $\omega_c = 1.5 \times 10^7$ s^{-1}. The initial electron bunch (an electron density of 1×10^8 cm^{-1} and the Langmuir frequency $\omega_b = 2.5 \times 10^8$ s^{-1}) had a cylindrical shape (the radius $r = 2$ cm and a duration of 6 ns) and was injected with an initial velocity of 3×10^7 m/s into plasma along the axis of the system. The initial length of the bunch was approximately equal to the wake wavelength in the background plasma.

4. Dynamics of a Short Bunch in Plasma in the Absence of a Magnetic Field

Now, let us consider the dynamics of an initially cylindrical electron bunch in the wakefield excited by itself

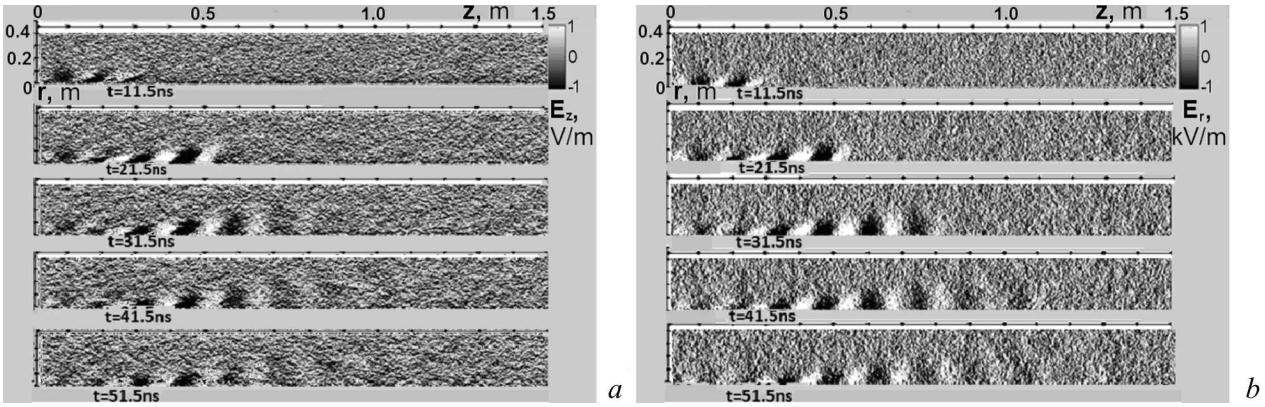

Fig. 2. Distributions of the longitudinal (a) and radial (b) components of the electric field excited by a short cylindrical bunch at $B = 0$

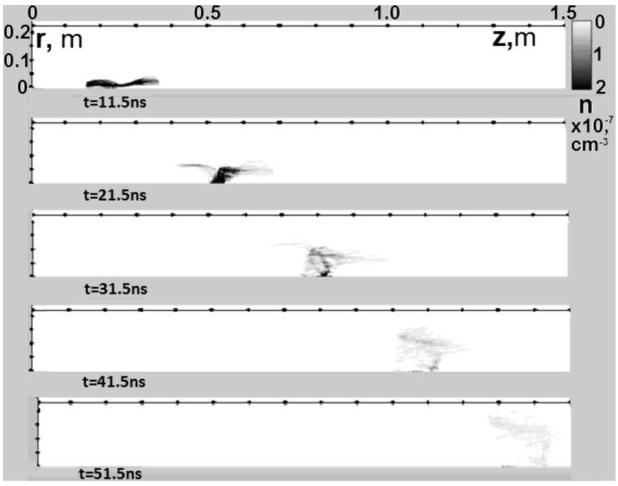

Fig. 3. Distribution of the electron density in a bunch at various stages of its flight through the system at $B = 0$

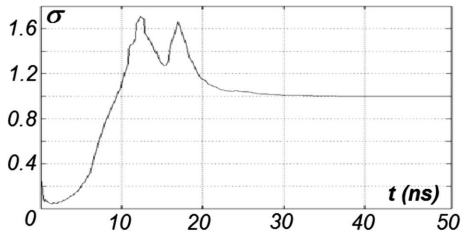

Fig. 4. Time dependence of the bunch deformation coefficient σ at $B = 0$

in the absence of external magnetic field. The spatial distributions of the components of the electric field excited by the bunch are shown in Fig. 2 for various time moments. One can see that just behind the bunch front edge, the longitudinal component of the field has a sign that corresponds to the deceleration of bunch electrons in the axial direction. The radial component sign corresponds to the acceleration of electrons in the direction away from the axis, i.e. to the radial defocusing. If moving away from the bunch front edge, the field components change their signs with a period that corresponds to the wake wavelength.

Figure 3 demonstrates the spatial distributions of the bunch density at various time moments. A comparison of Figs. 2 and 3 shows that the wakefield becomes mainly concentrated in the volume, through which the bunch moves, in accordance with the prediction of the analytical calculation for a wide bunch (for the model parameters $r/r_D \approx 40$). The radial swelling of the bunch results in that the width of the region, in which the wakefield is excited, becomes larger.

According to the wakefield character described above, the electrons at the front edge of the bunch are decelerated at the initial time moments, and their local density decreases. Simultaneously, they start to move away from the axis of the system to form a cavity at the bunch axis. The back half of the bunch corresponds to the accelerating phase of the longitudinal wakefield. As a result, the bunch becomes longitudinally concentrated in its central part, where the accelerated electrons from its back part and the decelerated electrons from its front part meet. The change in the sign of the radial field component leads to that the radial focusing occurs in approximately the same region.

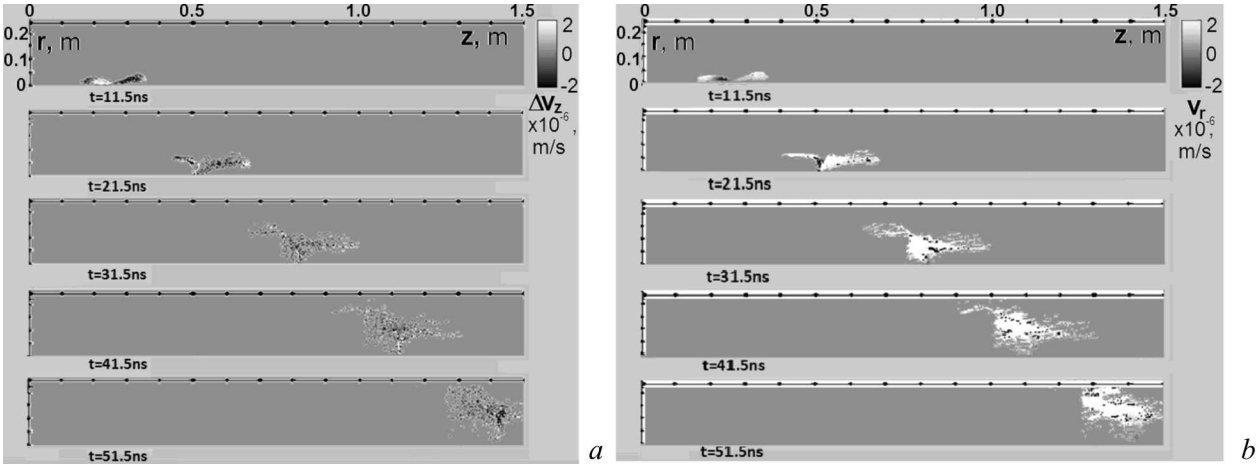

Fig. 5. Distributions of the longitudinal (a) and radial (b) components of the electron velocity in the bunch at various stages of its flight through the system at $B = 0$

As is seen from Fig. 3, the time moment, when the radial focusing is maximum, is close to $t = 10.5$ ns, and the time moment, when the longitudinal focusing is maximum, to $t = 21.5$ ns.

In the panel that corresponds to the time moment $t = 31.5$ ns, one can see that the particles in the central part of the bunch are already overtaken. At this time moment, the bunch, as a whole, looks like a funnel opened backward by an angle close to $\pi/2$. This moment corresponds to the change in the shape of the regions corresponding to the same sign of the wakefield in Fig. 2. Later, the density of electrons in the bunch becomes substantially lower.

In order to determine the time moments of the maximum radial and longitudinal focusings more accurately, let us introduce the coefficient of bunch deformation,

$$\sigma(t) = \frac{\int\limits_{-\infty}^{\infty} dz \int\limits_{0}^{\infty} 2\pi r dr [n(\mathbf{r},\mathbf{t}) - n_0(\mathbf{r})]^2}{\int\limits_{-\infty}^{\infty} dz \int\limits_{0}^{\infty} 2\pi r dr n_0^2(\mathbf{r})}, \qquad (9)$$

where $n_0(\mathbf{r})$ and $n(\mathbf{r},\mathbf{t})$ are the initial and current, respectively, distributions of the electron density in the bunch in the coordinate system moving with it. If the distribution of electrons in the bunch does not change in time, we have $\sigma = 0$. If the bunch becomes defocused and $n(\mathbf{r},\mathbf{t}) \to 0$, we obtain $\sigma \to 1$. Finally, at the time moments when the bunch is substantially focused, the deformation coefficient grows.

The time dependence of the deformation coefficient is plotted in Fig. 4. The first maximum (at $t = 12$ ns) corresponds to the maximum radial focusing of the bunch, and the second one (at $t = 17$ ns) to its maximum longitudinal focusing.

As a result of the processes described above, the spatial distribution of electrons in the front part of the bunch acquires a funnel-like shape (with the opening directed forward). Since the wakefield is excited by the most concentrated part of the bunch, the region of a steady wakefield phase acquires the same shape (Fig. 2).

In Fig. 5, the spatial distributions of the longitudinal and radial components of the electron velocity in the bunch at various time moments are depicted. In general, they correspond to the conclusions made on the basis of the spatial distributions of electric field components. Really, as one can see in the distribution at $t = 10.5$ ns, the front part of the bunch is mainly decelerated, whereas the back one is accelerated. However, in the region immediately adjacent to the front edge, the electrons are accelerated, whereas in the region adjacent to back edge, they are, on the contrary, decelerated. As for the radial velocity component, it is directed away from the axis of the system everywhere, but in the central bunch region.

Finally, in Fig. 6, the spatial distributions of the current density components in the background plasma are shown. One can see that, under the wakefield action, the electrons in the background plasma mainly oscillate in the radial direction.

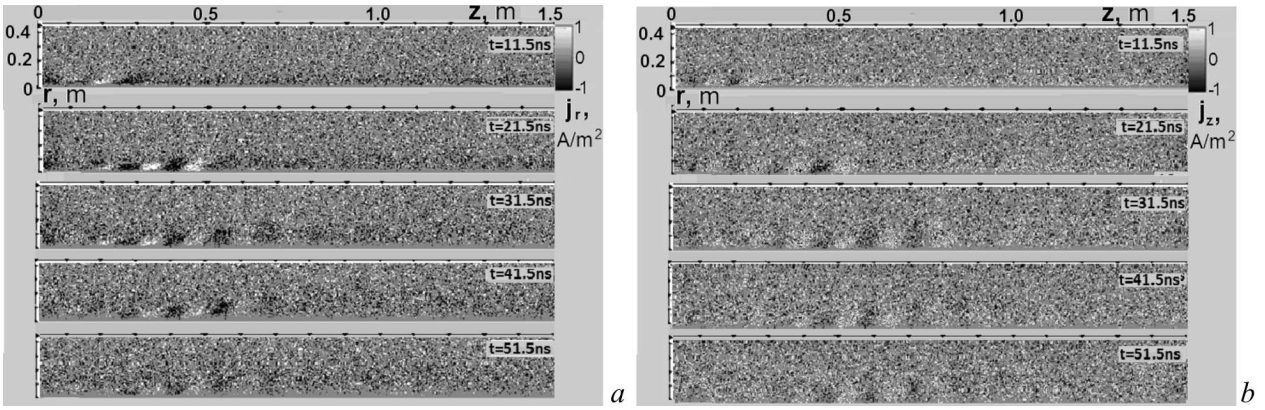

Fig. 6. Distributions of the radial (a) and longitudinal (b) components of the current density in the background plasma at $B = 0$

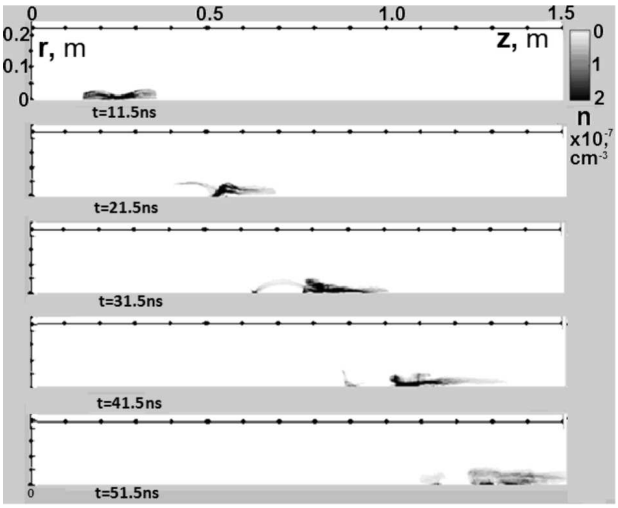

Fig. 7. Distributions of the electron density in the bunch at various stages of bunch flight through the system ($B = 1$ mT)

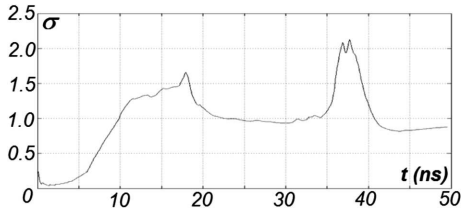

Fig. 8. Time dependence of the bunch deformation coefficient σ ($B = 1$ mT)

Hence, on the basis of simulation results, it is established that the dynamics of the electron bunch injected into plasma without the magnetic field is determined by excited wakefields. The regions of focusing and defocusing in the longitudinal and radial directions alternate [19]. The time moments that correspond to the maximum longitudinal and transverse focusings do not coincide in the general case. The electrons in the background plasma oscillate mainly in the radial direction under the wakefield action.

5. Excitation of Wakefields and the Dynamics of a Short Bunch in Plasma in the Presence of a Longitudinal Magnetic Field

Now, let us consider the influence of a longitudinal magnetic field on the wakefield excitation by electron bunches and the inverse effect of those wakefields on the bunch dynamics. Figure 7 demonstrates the spatial distributions of the electron density in a bunch at various time moments, provided that a longitudinal magnetic field is applied. A comparison of this figure with Fig. 3 testifies that the magnetic field, in general, suppresses the radial defocusing of the bunch. The electrons are mainly concentrated in the front half of the bunch. However, the total bunch length becomes a little longer at that. A comparison of the time dependences obtained for the coefficient of bunch deformation in the presence (Fig. 8) and absence (Fig. 4) of the magnetic field shows that the latter suppresses the effect of radial focusing (see a maximum at $t = 12$ ns in Fig. 4) produced by the wakefield. Instead, there arises a more pronounced maximum at $t = 37$ ns (cf. the bunch density distribution at $t = 41$ ns in Fig. 7), which can be associated with the magnetic focusing of the bunch.

The mechanism of this focusing is similar to the suppression of the bunch swelling by a longitudinal magnetic field. It is evident from Fig. 9, in which the spatial distributions of the velocity components for electrons in the bunch are depicted. The radial motion of electrons (Fig. 9, *b*), which is stimulated by the corresponding wakefield component, generates an azimuthal component of the Lorentz force in the longitudinal magnetic field. As a result, the electrons acquire an azimuthal velocity, with electrons in the middle part of the bunch and near the bunch edges rotating in opposite directions (Fig. 9, *c*). In turn, the azimuthal motion of electrons in the longitudinal magnetic field generates a radial component of the Lorentz force. Just the latter provides the radial focusing of those electrons that underwent the radial defocusing in the absence of magnetic field. One may expect that this focusing for the same bunch and, hence, the corresponding maximum of the bunch deformation coefficient will periodically repeat.

The non-zero longitudinal magnetic field, non-zero azimuthal velocity gradient, and formation of a cavity at the bunch axis (Fig. 7) can give rise, in principle, to the development of the diocotron instability and, accordingly, can violate the axial symmetry of the system. On the other hand, there is no cavity in the bunch at the initial time moment. The cavity shape considerably changes in time, which can prevent the development of this instability. Unfortunately, the 2.5-dimensional code used by us in calculations is inherently based on the axial symmetry of the system, so that it could not be used to study the probable evolution of the diocotron instability.

In Fig. 10, the spatial distributions of wakefield components excited in plasma with an applied longitudinal magnetic field are exhibited. A comparison with Fig. 2 demonstrates that the magnetic focusing of the bunch, which interferes its smearing, appreciably enlarges the region, where the bunch excites the wakefield [17]. Moreover, the amplitude of the wakefield electric field also increases a little. Note that the radius of the region occupied by the longitudinal field grows in the interval $z = 0.5 \div 0.8$ m, whereas the field intensity decreases here. In the interval $z = 0.8 \div 1$ m, the radius of this region decreases, whereas the field intensity increases. Comparing these features with Fig. 7, a conclusion can be drawn that they are induced by the processes of bunch defocusing and, afterward, its radial focusing by the magnetic field.

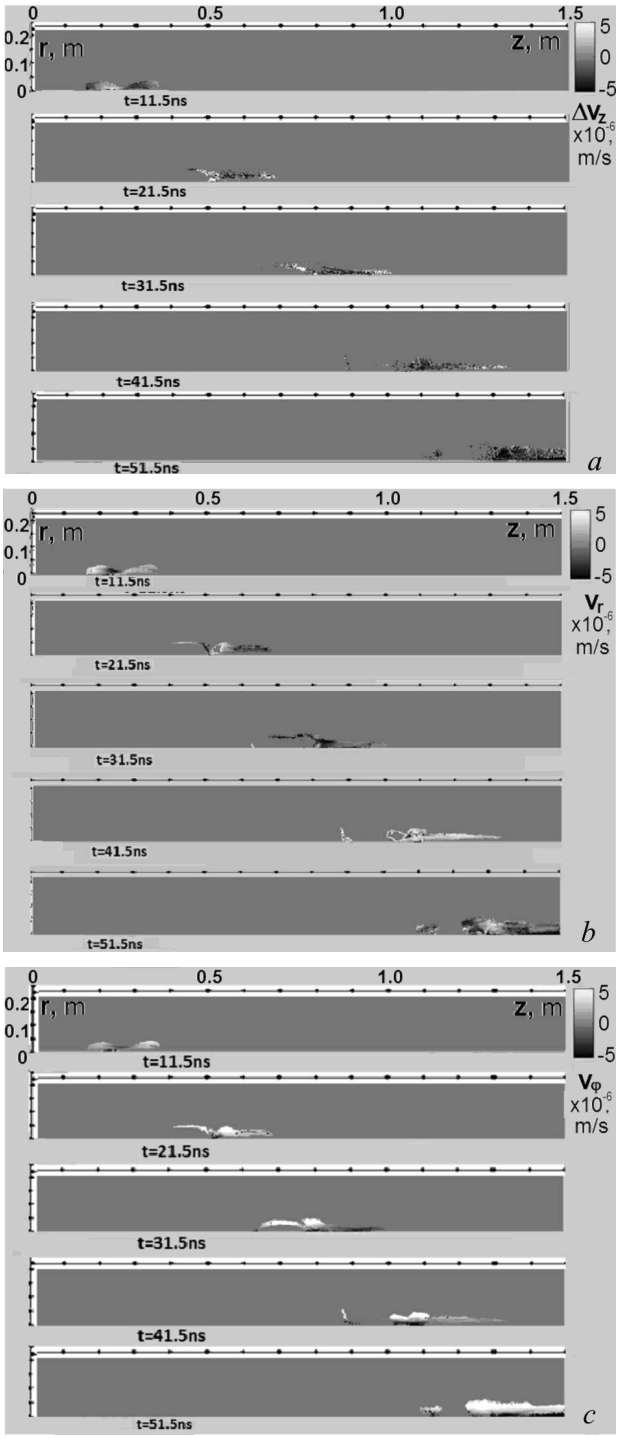

Fig. 9. Distributions of the longitudinal (a), radial (b), and azimuthal (c) velocity components of the bunch electrons at various stages of the bunch flight through the system ($B = 1$ mT)

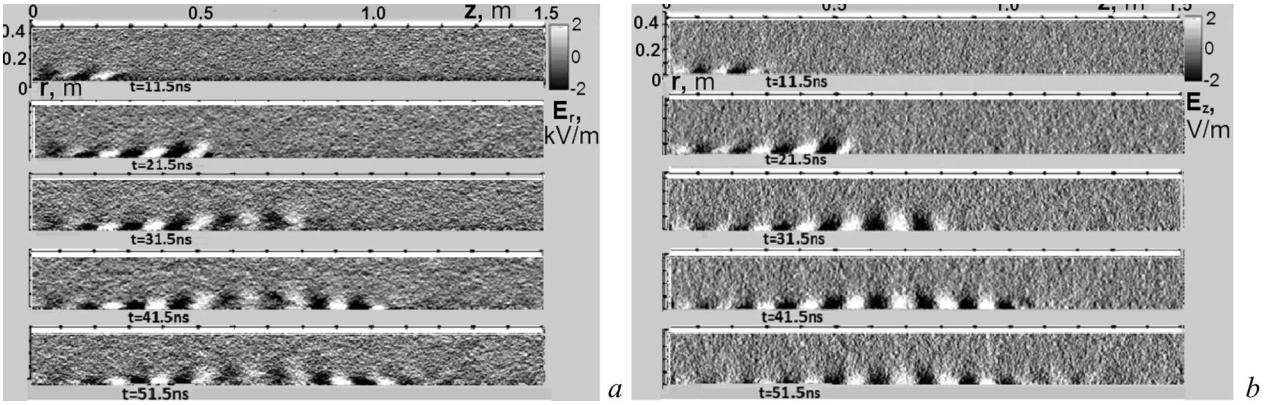

Fig. 10. Distributions of the radial (a) and longitudinal (b) electric field components for the external magnetic field $B = 1$ mT

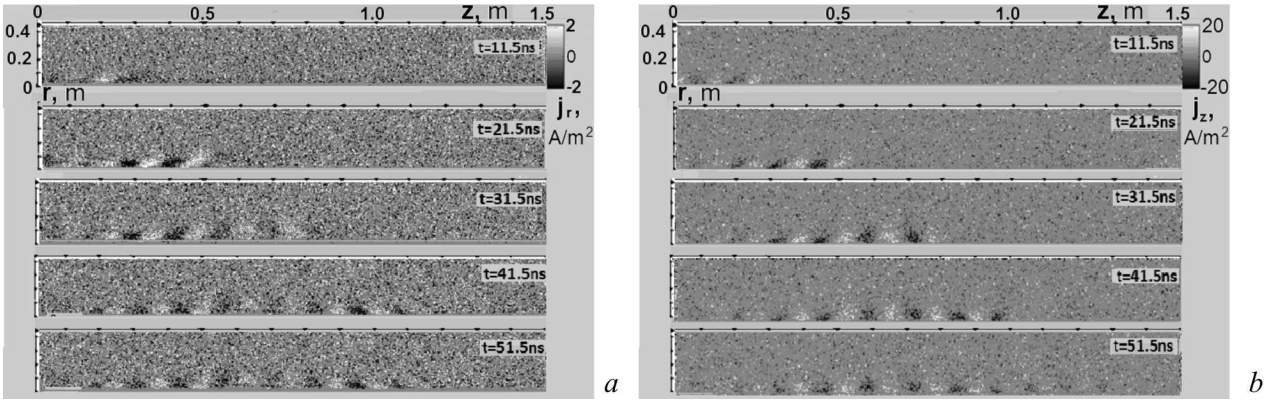

Fig. 11. Distributions of the radial (a) and longitudinal (b) current density components in the background plasma ($B = 1$ mT)

A comparison of Figs. 10 and 7 also shows that, irrespective of whether the magnetic field is present or not, the shape of the regions with a constant wakefield phase reproduces the shape of the most concentrated part in the electron bunch.

In Fig. 11, the spatial distributions of the current density components in the background plasma, which arise owing to the wakefield excitation, are exhibited. A comparison with Fig. 6 shows that the imposing of a longitudinal magnetic field results in that the oscillations of plasma electrons become mainly longitudinal. At the same time, without the magnetic field, the transverse electron oscillations dominate.

6. Conclusions

An external magnetic field directed along the axis of the system suppresses the radial defocusing of an electron bunch injected into plasma, but gives rise to its elongation. Accordingly, in the time dependence of the bunch deformation coefficient, there appears a second maximum (and, probably later, next maxima) associated with the radial focusing of the bunch in the magnetic field.

The mechanism of bunch focusing in the magnetic field is similar to the counteraction to the beam swelling in vacuum with the help of a longitudinal magnetic field. The radial motion of electrons in the bunch directed away from the axis of the system is induced by the corresponding wakefield component. In the longitudinal magnetic field, it generates the azimuthal component of the Lorentz force and, accordingly, the azimuthal component of the electron velocity. The azimuthal motion of electrons in a longitudinal magnetic field generates the radial component of the Lorentz force, which returns electrons to the axis of the system.

The longitudinal magnetic field gives rise to a broadening of the region, in which the bunch excites

the wakefield. The specific features in the spatial distribution of the latter are determined by the dynamics of the most concentrated bunch part.

The structure of currents in the background plasma is governed by the wakefield. The longitudinal magnetic field gives rise to an appreciable growth of the longitudinal current density component in comparison with the transverse one.

1. P. Chen, J.M. Dawson, R.W. Huff, and T. Katsouleas, Phys. Rev. Lett. **54**, 693 (1985).
2. M.J. Hogan, T.O. Raubenheimer, A. Seryi, P. Muggli, T. Katsoulеas, C. Huang, W. Lu, W. An, K.A. Marsh, W.B. Mori, C.E. Clayton, and C. Joshi, New J. Phys. **12**, 055030 (2010).
3. A. Tremaine, J. Rosenzweig, and P. Schoessow, Phys. Rev. E **56**, 7204 (1997).
4. V.I. Maslov and I.N. Onishchenko, Problems of Atomic Sci. and Techn. **4**, 69 (2013).
5. A. Bazzania, M. Giovannozzic, P. Londrillob, S. Sinigardia, and G. Turchettia, C. R. Mecanique **342**, 647 (2014).
6. A. Caldwell and K.V. Lotov, Phys. Plasmas **18**, 103101 (2011).
7. K.V. Lotov, Phys. Plasmas **20**, 083119 (2013).
8. L. Yi, B. Shen, K. Lotov, L. Ji, X. Zhang, W. Wang, X. Zhao, Y. Yu, J. Xu, X. Wang, Y. Shi, L. Zhang, T. Xu, and Zh. Xu, Phys. Rev. Special Topics – Accelerators and Beams **16**, 071301 (2013).
9. K.V. Lotov, V.I. Maslov, I.N. Onishchenko, and I.P. Yarovaya, Problems of Atomic Sci. and Techn. **4**, 73 (2013).
10. J. Vieira, Y. Fang, W.B. Mori, L.O. Silva, and P. Muggli, Phys. Plasmas **19**, 063105 (2012).
11. T. Tajima and J.M. Dawson, Phys. Rev. Lett. **43**, 267 (1979).
12. I. Blumenfeld, C.E. Clayton, F.J. Decker, M.J. Hogan, C. Huang *et al.*, Nature **445**, 741 (2007).
13. W. P. Leemans, A.J. Gonsalves, H.-S. Mao, K. Nakamura, C. Benedetti, C.B. Schroeder *et al.*, Phys. Rev. Lett. **113**, 245002 (2014).
14. V.I. Maslov, I.N. Onishchenko, O.M. Svystun, and V.I. Tkachenko, in *International Young Scientists Forum on Applied Physics, Dnipropetrovsk, Ukraine, September 29–October 2, 2015*, report NPP-5.
15. I.O. Anisimov and K.I. Lyubich, J. Plasma Phys. **66**, 157 (2001).
16. V.P. Kovalenko, Usp. Fiz. Nauk **139**, 223 (1983).
17. M.A. Shcherbinin and I.O. Anisimov, Problems of Atomic Sci. and Techn. **94**, 116 (2014).
18. Yu.M. Tolochkevych, I.O. Anisimov, and T.E. Litoshenko, Ukr. J. Phys. **60**, 16 (2014).
19. V.A. Balakirev, V.I. Karas', I.V. Karas', Fiz. Plazmy **28**, 144 (2002).

Received 07.05.16.
Translated from Ukrainian by O.I. Voitenko

І.О. Анісімов, М.А. Щербінін

ДИНАМІКА КОРОТКИХ ЕЛЕКТРОННИХ ЗГУСТКІВ ТА ЗБУДЖЕНИХ НИМИ КІЛЬВАТЕРНИХ ПОЛІВ У ПЛАЗМІ ЗА ВІДСУТНОСТІ ТА ЗА НАЯВНОСТІ ПОЗДОВЖНЬОГО МАГНІТНОГО ПОЛЯ

Р е з ю м е

За допомогою комп'ютерного моделювання розглянуто вплив поздовжнього магнітного поля на збудження кільватерних полів у плазмі первісно циліндричним електронним згустком, довжина якого дорівнює довжині кільватерної хвилі, й зворотний вплив збуджуваних полів на динаміку згустка. Показано, що таке магнітне поле може зменшити радіальне дефокусування згустка і збільшити довжину області, в якій збуджуються кільватерні хвилі, і амплітуду цих хвиль.